MIT–CTP 3967 SLAC–PUB–13355 UCLA/08/TEP/26 Saclay-IPhT–T08/123

One-Loop Multi-Parton Amplitudes with a Vector Boson for the LHC

C. F. Berger[a], Z. Bern[b*], L. J. Dixon[c], F. Febres Cordero[b], D. Forde[b,c], H. Ita[b], D. A. Kosower[d] and D. Maître[c]

[a] *Center for Theoretical Physics, Massachusetts Institute of Technology, Cambridge, MA 02139, USA*

[b] *Department of Physics and Astronomy, UCLA, Los Angeles, CA 90095-1547, USA*

[c] *Stanford Linear Accelerator Center, Stanford University, Stanford, CA 94309, USA*

[d] *Institut de Physique Théorique, CEA–Saclay, F–91191 Gif-sur-Yvette cedex, France*

In this talk, we present the first, numerically stable, results for the one-loop amplitudes needed for computing $W, Z + 3$ jet cross sections at the LHC to next-to-leading order in the QCD coupling. We implemented these processes in BlackHat, an automated program based on on-shell methods. These methods scale very well with increasing numbers of external partons, and are applicable to a wide variety of problems of phenomenological interest at the LHC.

Particle physicists eagerly await the new physics, beyond the Standard Model, that is expected to emerge at the LHC. In many cases, the Standard Model will produce background events that can obscure the signals of new physics. Uncovering and understanding these signals will make use of detailed kinematic constraints (such as several identified jets, cuts on missing transverse energy, etc.) and reliable predictions for background processes.

Leading-order cross sections in QCD suffer from large uncertainties, and do not suffice for quantitative knowledge of backgrounds. Next-to-leading order (NLO) corrections lead to a significant improvement. As reviewed in ref. [1], there are a large number of processes of interest involving many final-state jets. Developing methods for computing such processes has involved a dedicated effort over many years, also described in ref. [1]. The main bottleneck to NLO computations with four or more final-state objects (including jets) has been in evaluating one-loop (virtual) corrections. In this writeup we present results from BlackHat [2], which is one of a new generation of programs based on on-shell methods. Other numerical efforts along similar lines are described in refs. [3, 4, 5]. These methods [3, 6, 7, 8, 9, 10, 11, 12, 13, 14] offer excellent scaling properties as the number of external legs increases, promising a general solution to the problem of calculating one-loop amplitudes with a large number of final state partons.

BlackHat is an automated program generating numerical values for one-loop amplitudes at given kinematic points. The on-shell formalism it uses is distinct from Feynman diagrams. The latter are inherently gauge non-invariant, allowing unphysical states to circulate in the loops. Large gauge-dependent cancellations between terms make a conventional diagrammatic approach impractical and numerically unstable for sufficiently many external states. (Analytically, the conventional approach suffers from an explosion in intermediate-stage computational complexity even with only a modest increase in number of external legs.) On-shell methods bypass these cancellations by building new amplitudes using only simpler on-shell amplitudes as input. BlackHat has been validated for one-loop six-, seven- and eight-gluon amplitudes, demonstrating excellent speed and numerical stability [2]. In this talk we present results for the leading-color contributions to one-loop $qggg\bar{q}V$ amplitudes, where the vector boson V decays into a pair of leptons. Sample diagrams for these amplitudes are shown in fig. 1(b). This is a key contribution to NLO corrections to vector boson (γ^*, W, or Z) production in association with three jets, which is an important background to searches for supersymmetry [15]. Here we present 'primitive' amplitudes, which can be converted easily to amplitudes for any choice of V, by multiplying by appropriate propagator and coupling-constant factors [8].

On-shell methods use the unitarity and factorization properties of amplitudes in quantum field theories to systematically construct amplitudes with larger numbers of loops or legs. Terms with branch cuts can be determined by evaluating unitarity cuts in four dimensions. The unitarity method [6] provides a systematic means for constructing these terms directly from tree amplitudes. Recent refinements [3, 9, 11, 13], exploiting complex momenta, greatly

* Presenter at 34th International Conference on High Energy Physics, Philadelphia, USA, July 2008.

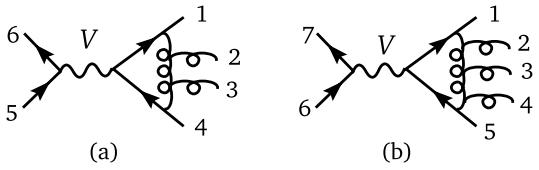

FIG. 1: Sample leading-color diagrams for the amplitudes (a) $qggg\bar{q}\bar{l}l$ and (b) $qgggg\bar{q}\bar{l}l$. The leptons, $\bar{l}, l$ couple to the quarks via a vector boson, V. Analytic expressions for the six-point amplitudes (a) are given in ref. [8].

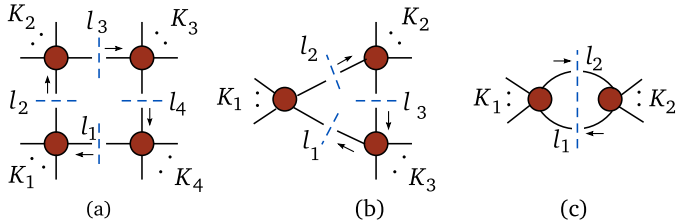

FIG. 2: The quadruple (a), triple (b) and double (c) cuts used to evaluate the coefficients of the box, triangle and bubble integral functions. The momentum of a cut line satisfies the on-shell conditions, $l_j^2 = m_j^2$, where m_j is the mass of the cut line.

enhance the effectiveness of generalized (multiple) cuts [8]. By restricting the momenta of the cut lines to four dimensions we may use powerful spinor formalisms. This procedure drops rational terms, which could be retained by evaluating the cuts in D dimensions [5, 7]. Alternatively we can extract the rational terms using on-shell recursion, developed by Britto, Cachazo, Feng and Witten at tree level [16], and extended to loop level in refs. [10, 12].

Any dimensionally-regulated one-loop amplitude, with four-dimensional external momenta, may be written as,

$$A_n = \sum_i d_i I_4^i + \sum_i c_i I_3^i + \sum_i b_i I_2^i + R_n + \mathcal{O}(\epsilon)\,. \tag{1}$$

The scalar integrals $I_{2,3,4}$, respectively bubbles, triangles, and boxes, are known functions [17] and contain all the amplitude's branch cuts. (If massive particles propagate in the loops there are also tadpole contributions.) The coefficients of these integrals, b_i, c_i, and d_i, are rational functions of the external momenta, which may be extracted from generalized unitarity cuts using four-dimensional values for the loop momenta. The remaining function, R_n, is also rational and is computed in BlackHat using on-shell recursion.

The box integral coefficients are the most straightforward to compute. Imposing four on-shell conditions on a one-loop integrand, as shown in fig. 2(a), while keeping the loop momentum in four dimensions, freezes the integration completely. This procedure isolates the coefficient of a single box integral uniquely, allowing for a simple evaluation [9]. The coefficient is given by the product of four tree amplitudes at the corners of the box,

$$d_i \;=\; \frac{1}{2} \sum_{\sigma=\pm} A^{\rm tree}_{(1)} A^{\rm tree}_{(2)} A^{\rm tree}_{(3)} A^{\rm tree}_{(4)} \Big|_{l_j = l_j^{(\sigma)}}\,, \tag{2}$$

where the cut loop momenta $l_j^{(\pm)}$ are the two solutions to the quadruple-cut on-shell conditions.

Triangle coefficients are obtained from the triple cuts shown in fig. 2(b). Here, the cut conditions no longer freeze the integration completely; one degree of freedom is left over. To evaluate the triangle coefficient we use the analytic parametrization method of Forde [13], along with the Ossola, Papadopoulos and Pittau [3] procedure of subtracting previously-computed box contributions from the triple cut. This eliminates unwanted poles from the complex plane, rendering the computation of these coefficients more numerically stable. For the case of bubble coefficients, two degrees of freedom remain after imposing two cut conditions, as shown in fig. 2(c). We refer the reader to refs. [2, 3, 13] for details. Spinor-based methods have also been developed for computing triangle and bubble coefficients analytically [11].

At most phase-space points, ordinary double-precision arithmetic suffices to obtain a relative accuracy of 10^{-5} or better, even for the most complicated of the amplitudes. This is far better than is needed in a realistic NLO calculation, given all the other uncertainties. Nonetheless, for a small percentage of phase-space points, numerical instabilities due to roundoff error do arise, because of large cancellations between different terms in eq. (1). Such points typically feature numerically small values for a Gram determinant. To identify these points dynamically we require that all spurious singularities cancel amongst bubble coefficients, and that the known coefficient of the $1/\epsilon$

TABLE I: Numerical results for leading-color amplitudes with an intermediate vector boson at the six- and seven-point momenta given in eqs. (9.1) and (9.3) of ref. [12] (for renormalization scale $\mu = 6$ and 7, respectively). The numerical values for the six-point amplitudes agree with the analytic results of ref. [8]. Our helicity labels follow an all-outgoing convention. The three values on each line are the $1/\epsilon^2$, $1/\epsilon$ and finite contributions to the amplitudes, normalized by the tree amplitude.

Helicity	$1/\epsilon^2$	$1/\epsilon$	ϵ^0
$1_q^+ 2_g^+ 3_g^+ 4_{\bar{q}}^- 5_{\bar{l}}^- 6_l^+$	-3.00000	$-5.86428 - i\,6.28319$	$-7.50750 - i\,12.90848$
$1_q^+ 2_g^+ 3_g^- 4_{\bar{q}}^- 5_{\bar{l}}^- 6_l^+$	-3.00000	$-5.86428 - i\,6.28319$	$0.10598 - i\,11.74860$
$1_q^+ 2_g^-, 3_g^+ 4_{\bar{q}}^- 5_{\bar{l}}^- 6_l^+$	-3.00000	$-5.86428 - i\,6.28319$	$1.37392 - i\,14.17999$
$1_q^+ 2_g^+ 3_g^+ 4_g^+ 5_{\bar{q}}^- 6_{\bar{l}}^- 7_l^+$	-4.00000	$-10.43958 - i\,9.42478$	$2.10030 - i\,33.97042$
$1_q^+ 2_g^+ 3_g^+ 4_g^- 5_{\bar{q}}^- 6_{\bar{l}}^- 7_l^+$	-4.00000	$-10.43958 - i\,9.42478$	$-9.25860 - i\,33.31407$
$1_q^+ 2_g^- 3_g^+ 4_g^+ 5_{\bar{q}}^- 6_{\bar{l}}^- 7_l^+$	-4.00000	$-10.43958 - i\,9.42478$	$-5.51046 - i\,33.55522$
$1_q^+ 2_g^- 3_g^+ 4_g^- 5_{\bar{q}}^- 6_{\bar{l}}^- 7_l^+$	-4.00000	$-10.43958 - i\,9.42478$	$-6.36853 - i\,29.29380$

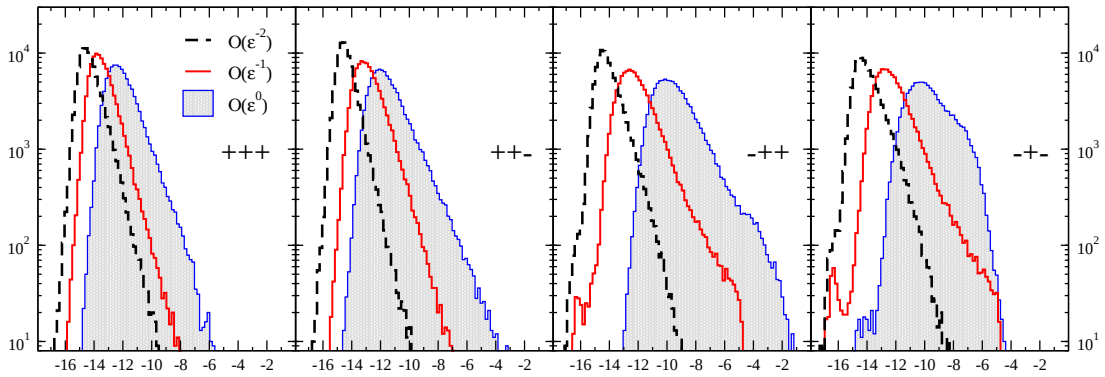

FIG. 3: The distribution of the logarithm of the relative error over 100,000 phase-space points, for four independent helicity choices for the $qggg\bar{q}\bar{l}l$ leading color amplitudes. The helicity labels on the plots indicate the helicities of the three gluons. The dashed (black) curve in each histogram gives the relative error for the $1/\epsilon^2$ part, the solid (red) curve gives the $1/\epsilon$ singularity, and the shaded (blue) distribution gives the finite ϵ^0 component of the corresponding helicity amplitude.

singularity generated by bubble integrals be correct. Whenever the result at a given point fails these criteria, we recalculate the amplitude at higher precision. In practice, this step has only a modest impact on the overall speed of the program, given the small fraction of unstable points.

To test the implementation of vector-boson amplitudes in BlackHat, we first evaluated the $qggg\bar{q}\bar{l}l$ one-loop primitive amplitudes given in eqs. (8.4)–(8.19) of ref. [8]. A sample diagram for these primitive amplitudes is shown in fig. 1(a). The amplitudes; values from BlackHat, at the phase-space point in eq. (9.1) of ref. [12], are presented on the first three lines of table I. We have normalized the values by dividing by the corresponding tree amplitudes. Similarly, at the phase-space point in eq. (9.3) of ref. [12], we compute the primitive amplitudes with one additional gluon, shown in fig. 1(b), with the results displayed on the final four lines of table I. (We remove the universal prefactor, $c_\Gamma = \Gamma(1+\epsilon)\Gamma^2(1-\epsilon)/[(4\pi)^{2-\epsilon}\Gamma(1-2\epsilon)]$, where $\epsilon = (4-D)/2$, from the evaluation.)

To assess the numerical stability of BlackHat, we evaluated the amplitudes in table I at 100,000 phase-space points drawn from a flat distribution, taking the quark and gluon labeled by 1 and 2 as the incoming partons. (We impose the following cuts: $E_T > 0.01\sqrt{s}$, $\eta < 3$, and $\Delta_R > 0.4$.) The histograms in fig. 3 show the results for the seven-point amplitudes. The horizontal axis gives the logarithmic relative error, $\log_{10}(|A_n^{\rm num} - A_n^{\rm target}|/|A_n^{\rm target}|)$, for each of the $1/\epsilon^2$, $1/\epsilon$, and ϵ^0 parts of the one-loop amplitude. For the seven-point target—where no previous results are available—we used quadruple-double (~ 64 digits) precision results evaluated in BlackHat. The vertical axis in these plots shows the number of phase-space points in a bin that agree with the target to a specified relative

precision. The vertical scale is logarithmic, which enhances the visibility of the tail of the distribution, illustrating the good numerical stability.

In summary, in this talk we presented the first, numerically stable evaluation of the leading-color virtual matrix elements needed for the NLO corrections to $pp \to V + 3$ jets, including vector boson decay to a pair of leptons. The subleading-color contributions can be computed in a similar manner. A key remaining task is to interface BlackHat with an automated program [18] for combining real and virtual matrix elements, in order to produce NLO cross sections for phenomenologically important multi-jet processes at the LHC.

We thank Academic Technology Services at UCLA for computer support. This research was supported by the US Department of Energy under contracts DE–FG03–91ER40662, DE–AC02–76SF00515 and DE–FC02–94ER40818. DAK's research is supported by the Agence Nationale de la Recherce of France under grant ANR–05–BLAN–0073–01. The work of DM was supported by the Swiss National Science Foundation (SNF) under contract PBZH2–117028.

[1] Z. Bern *et al.*, 0803.0494 [hep-ph].

[2] C. F. Berger *et al.*, 0803.4180 [hep-ph].

[3] G. Ossola, C. G. Papadopoulos and R. Pittau, Nucl. Phys. B **763**, 147 (2007) [hep-ph/0609007].

[4] R. K. Ellis, W. T. Giele and Z. Kunszt, JHEP **0803**, 003 (2008) [0708.2398 [hep-ph]]; G. Ossola, C. G. Papadopoulos and R. Pittau, JHEP **0803**, 042 (2008) [0711.3596 [hep-ph]]; P. Mastrolia, G. Ossola, C. G. Papadopoulos and R. Pittau, JHEP **0806**, 030 (2008) [0803.3964 [hep-ph]]; T. Binoth, G. Ossola, C. G. Papadopoulos and R. Pittau, JHEP **0806** (2008) 082 [0804.0350 [hep-ph]]; W. T. Giele and G. Zanderighi, 0805.2152 [hep-ph].

[5] W. T. Giele, Z. Kunszt and K. Melnikov, JHEP **0804**, 049 (2008) [0801.2237 [hep-ph]]; G. Ossola, C. G. Papadopoulos and R. Pittau, 0802.1876 [hep-ph]; R. K. Ellis, W. T. Giele, Z. Kunszt and K. Melnikov, 0806.3467 [hep-ph].

[6] Z. Bern, L. J. Dixon, D. C. Dunbar and D. A. Kosower, Nucl. Phys. B **425**, 217 (1994) [hep-ph/9403226]; Nucl. Phys. B **435**, 59 (1995) [hep-ph/9409265].

[7] Z. Bern and A. G. Morgan, Nucl. Phys. B **467**, 479 (1996) [hep-ph/9511336]; Z. Bern, L. J. Dixon and D. A. Kosower, Ann. Rev. Nucl. Part. Sci. **46**, 109 (1996) [hep-ph/9602280]; Z. Bern, L. J. Dixon, D. C. Dunbar and D. A. Kosower, Phys. Lett. B **394**, 105 (1997) [hep-th/9611127]; Z. Bern, L. J. Dixon and D. A. Kosower, JHEP **0001**, 027 (2000) [hep-ph/0001001]; A. Brandhuber, S. McNamara, B. J. Spence and G. Travaglini, JHEP **0510**, 011 (2005) [hep-th/0506068]; C. Anastasiou, R. Britto, B. Feng, Z. Kunszt and P. Mastrolia, Phys. Lett. B **645**, 213 (2007) [hep-ph/0609191]; JHEP **0703**, 111 (2007) [hep-ph/0612277]; R. Britto and B. Feng, Phys. Rev. D **75**, 105006 (2007) [hep-ph/0612089]; R. Britto and B. Feng, JHEP **0802**, 095 (2008) [0711.4284 [hep-ph]]; R. Britto, B. Feng and P. Mastrolia, 0803.1989 [hep-ph]; R. Britto, B. Feng and G. Yang, 0803.3147 [hep-ph]; B. Feng and G. Yang, 0806.4016 [hep-ph]; S. D. Badger, 0806.4600 [hep-ph].

[8] Z. Bern, L. J. Dixon and D. A. Kosower, Nucl. Phys. B **513**, 3 (1998) [hep-ph/9708239].

[9] R. Britto, F. Cachazo and B. Feng, Nucl. Phys. B **725**, 275 (2005) [hep-th/0412103].

[10] Z. Bern, L. J. Dixon and D. A. Kosower, Phys. Rev. D **71**, 105013 (2005) [hep-th/0501240]; Phys. Rev. D **72**, 125003 (2005) [hep-ph/0505055]; Phys. Rev. D **73**, 065013 (2006) [hep-ph/0507005].

[11] R. Britto, E. Buchbinder, F. Cachazo and B. Feng, Phys. Rev. D **72**, 065012 (2005) [hep-ph/0503132]; R. Britto, B. Feng and P. Mastrolia, Phys. Rev. D **73**, 105004 (2006) [hep-ph/0602178]; P. Mastrolia, Phys. Lett. B **644**, 272 (2007) [hep-th/0611091].

[12] C. F. Berger, Z. Bern, L. J. Dixon, D. Forde and D. A. Kosower, Phys. Rev. D **74**, 036009 (2006) [hep-ph/0604195].

[13] D. Forde, Phys. Rev. D **75**, 125019 (2007) [0704.1835 [hep-ph]].

[14] Z. Bern, L. J. Dixon and D. A. Kosower, Annals Phys. **322**, 1587 (2007) [0704.2798 [hep-ph]].

[15] C. Buttar *et al.*, hep-ph/0604120.

[16] R. Britto, F. Cachazo and B. Feng, Nucl. Phys. B **715**, 499 (2005) [hep-th/0412308]; R. Britto, F. Cachazo, B. Feng and E. Witten, Phys. Rev. Lett. **94**, 181602 (2005) [hep-th/0501052].

[17] G. 't Hooft and M. J. G. Veltman, Nucl. Phys. B **153**, 365 (1979); G. J. van Oldenborgh and J. A. M. Vermaseren, Z. Phys. C **46**, 425 (1990); W. Beenakker and A. Denner, Nucl. Phys. B **338**, 349 (1990); A. Denner, U. Nierste and R. Scharf, Nucl. Phys. B **367**, 637 (1991); R. K. Ellis and G. Zanderighi, JHEP **0802**, 002 (2008) [0712.1851 [hep-ph]].

[18] T. Gleisberg and F. Krauss, Eur. Phys. J. C **53**, 501 (2008) [0709.2881 [hep-ph]]; M. H. Seymour and C. Tevlin, 0803.2231 [hep-ph]; K. Hasegawa, S. Moch and P. Uwer, 0807.3701 [hep-ph].